

# Polyethylene battery separator with auto-shutdown ability, thermal stability of 220°C, and hydrophilic surface via solid-state ultraviolet irradiation

Xiang Gao,<sup>1</sup> Wei Sheng,<sup>1</sup> Yongchang Wang,<sup>2</sup> Yegang Lin,<sup>1,3</sup> Yingwu Luo,<sup>1</sup> Bo-Geng Li<sup>1</sup>

<sup>1</sup>The State Key Laboratory of Chemical Engineering, College of Chemical and Biological Engineering, Zhejiang University, Hangzhou, China

<sup>2</sup>Zhejiang Province Institute of Energy and Nuclear Technology, Hangzhou, China

<sup>3</sup>Zhejiang Boer Plastic Co., Ltd., Wenzhou, China

Correspondence to: X. Gao (E-mail: gaox@zju.edu.cn)

**ABSTRACT:** To assure the safety of the lithium-ion battery, the separator is required to have good thermal stability. Because the single-layer polyethylene (PE) separator can only tolerate a temperature of 130°C, it is seldom employed currently by lithium-ion battery manufacturers although its cost is low. In this article, we modified PE separator chain structure through solid-state ultraviolet (UV) irradiation method to achieve a separator with composite structure of ~40% crystallized PE and ~70% gel content. Approximately 40% crystallized PE chains fulfill the task of auto-shutdown at 130°C through melting and filling the pores. At the same time, the PE separator can maintain integrity till 220°C because of its highly cross-linked chain structure. Besides, the modified PE separator is hydrophilic with a water contact angle of 33° after UV treatment and is able to absorb more electrolyte. However, the tensile strength and elongation at the break decreased because the cross-linking network increased the rigidity. Nevertheless, these values still meet the requirements as the separator for lithium-ion battery. Considering the low cost and easy preparation, current cross-linked PE separator has potential to be used in lithium-ion batteries for various applications, including electric vehicles and energy storage purpose. © 2015 Wiley Periodicals, Inc. *J. Appl. Polym. Sci.* **2015**, *132*, 42169.

**KEYWORDS:** batteries and fuel cells; cross-linking; membranes

Received 14 January 2015; accepted 2 March 2015

DOI: 10.1002/app.42169

## INTRODUCTION

Safety is of the first importance for lithium-ion batteries. As a result, besides many studies focusing on the electrodes of lithium-ion batteries to increase the energy density, power, etc., the efforts to increase thermal stability of the separator have never stopped because a separator with good thermal stability is especially important in avoiding serious accident happening to lithium-ion batteries, especially those with high capacity in the applications of electric vehicles or energy storage.<sup>1–3</sup>

The main safety jeopardy to the lithium-ion battery lies in the inside flammable organic electrolyte solution, which will cause fire and explosion at high temperature, mostly higher than 170°C.<sup>4,5</sup> Such an abnormal temperature usually arises from the failure of the separator in the battery. Due to various reasons, e.g., the perforation of separator caused by lithium dendrite growth, the abuse of battery, defects introduced in the manufacture process, etc., the separator may break locally causing the direct contact of the cathode and anode. This internal short cir-

cuit will cause the temperature increasing and enlarge the failure area of the separator. This vicious cycle may increase the temperature of the battery above the temperature that the separator can tolerate. The entire failure of the separator will cause the direct contact of the cathode and anode, which may cause serious fire or explosion. As a result, a separator with good thermal stability which can help avoiding the whole failure at abnormally high temperature is greatly desired.

Currently, the most widely used separators are polyolefin membranes, including polyethylene (PE), polypropylene (PP) single-layer separators, and PP/PE/PP triple-layer separator.<sup>6,7</sup> Among them the single-layer PE separator has low cost and was ever widely used in lithium-ion battery. However, its heat resistance ability is very poor. The melting temperature of PE is 130°C, which means a battery employing single-layer PE separator can only tolerate a temperature of 130°C at maximum. Above this temperature, the whole failure of the separator will occur and serious accident may happen. As a result, currently single-layer PE separators are seldom used in the lithium-ion batteries with

high capacity for electric vehicles or energy storage purpose. The PP/PE/PP triple-layer separator is more widely employed now because it gives the battery auto-shutdown capability. Under special conditions, the local internal short circuit may increase local temperature to 130°C. Then the middle PE layer will melt, stopping the transportation of lithium ions locally to avoid the further increase of the temperature. The PP layers can still assure the integrity of the separator, separating the electrodes till 160°C to avoid larger area contact of electrodes and uncontrollable temperature increase. As a result, a 30°C safety window increases the safety of lithium-ion batteries significantly. Nowadays, it is widely accepted that the auto-shutdown ability is necessary for the separator in lithium-ion battery. However, the triple-layer separator has higher cost and larger thickness compared with the single-layer separator. Furthermore, this 30°C safety window may not work effectively to stop the thermal runaway before the whole failure of the separator, i.e., 160°C is not high enough to guarantee the integrity of the separator in thermal runaway. An ideal separator should have auto-shutdown ability at a temperature above working temperature. The heat resistance temperature should be as high as possible to give a larger safety window. According to current studies, heat resistance of at least 200°C is preferred to help avoid serious accident.<sup>8–10</sup> Besides, it should be as thin as possible to achieve high energy density. And of course, the cost should be as low as possible considering that the high price of lithium-ion batteries is one of the blocks for the wide application of electric vehicles. Based on these considerations, many studies have been carried out to increase the thermal stability of the separator.<sup>11</sup> So far the ceramic separator, mostly PE separator coated with ceramic, is most successful one because it can tolerate a temperature much higher than 160°C but still has the auto-shutdown ability at around 130°C.<sup>12–15</sup> In spite of its wide applications, it has disadvantages such as the higher cost and increased thickness due to ceramic coating.

Another well-known method to increase the thermal stability of PE materials is through cross-linking.<sup>16</sup> By now a couple of studies have been carried out to cross-link the PE separator through electron beam irradiation,<sup>17–19</sup>  $\gamma$ -ray radiation,<sup>20</sup> etc. The thermal stability was truly increased compared with untreated PE separator. However, none of them can tolerate a temperature close to 200°C. The degradation of PE and the radiation effect on the porous structure of the PE separator are problems. So far there seems that no efforts were further carried out to resolve the thermal stability problem of the PE separator through cross-linking. Currently the single-layer PE separator is seldom employed in the preparation of the batteries with high capacity. However, this article will demonstrate the partially cross-linked single-layer PE separator obtained through well-controlled solid-state ultraviolet (UV) irradiation could meet those rigorous requirements by lithium-ion batteries.

## EXPERIMENTAL

### Materials

The commercial single-layer microporous PE separator with a thickness of 25  $\mu\text{m}$ , obtained from Asahi Kasai, was used for further modification. The commercial triple-layer PP/PE/PP

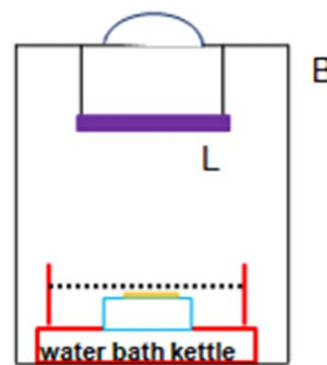


**Figure 1.** Schematic diagram of the irradiation device. [Color figure can be viewed in the online issue, which is available at [wileyonlinelibrary.com](http://wileyonlinelibrary.com).]

microporous separator with a thickness of  $\sim 38 \mu\text{m}$  was from Celgard LLC for comparison. Benzophenone (Aladdin, >98%) and triallylicyanurate (Aladdin, >98%) were used as photoinitiator and cross-linker, respectively. All the commercial reagents were used as received unless stated otherwise.

### Sample Irradiation Procedure

UV irradiation was carried out in a UV cure reactor constructed in the laboratory and shown schematically in Figure 1. B is an irradiation box. The high-pressure mercury lamp L, Phillips TUV 1000 W high-pressure mercury vapor lamp with most of the output at 153.7  $\mu\text{m}$ , was 10 cm away from the surface of the separator. During the irradiation, the separator was submerged in the water to maintain certain temperature. The irradiation tank is a water bath kettle (Electro Thermostatic Water Bath). A customized quartz container with the separator clipped in it was put in the bath. The water in the bath just submerged the separator.

### Characterization

**Gel Content.** After being irradiated, the samples were cut into thin slices and placed in a basket made of 200 mesh stainless-steel net. The gel content of the samples was determined through extracting the irradiated sample ( $w_1$ ) in the basket for 48 h with boiling xylene stabilized by 0.2% antioxidant of tinuvin144 and nitrogen protection to prevent oxidation. After extraction, the basket with samples was washed with acetone. After the samples were dried in the vacuum desiccator at about 70° to constant weight, the insoluble residue ( $w_2$ ) was weighed. The average gel content (wt %) in the test was calculated as  $100 \times (w_2/w_1)$ .

**Differential Scanning Calorimetry (DSC).** DSC measurements were carried out in a Perkin Elmer Pyris I calorimeter (DSC 7), programmed for a heat–hold–cool–heat cycle. The heating/cooling rate was 10°/min and the temperature range was 20–200° with a 1 min hold time. The crystallinity,  $X_c$ , was calculated by the relative ratio of fusion heat per gram of samples to the fusion heat of PE crystal (287.3 J/g).

**Thermogravimetric Analysis.** TGA was performed in a Shimadzu TGA-50H thermoanalyzer at a scan rate of 10°/min under the air flow rate of  $2 \times 10^{-5} \text{ m}^3/\text{min}$ .

**Mechanical Strength.** The mechanical strength was measured by a universal testing machine (Instron1185) at the temperature

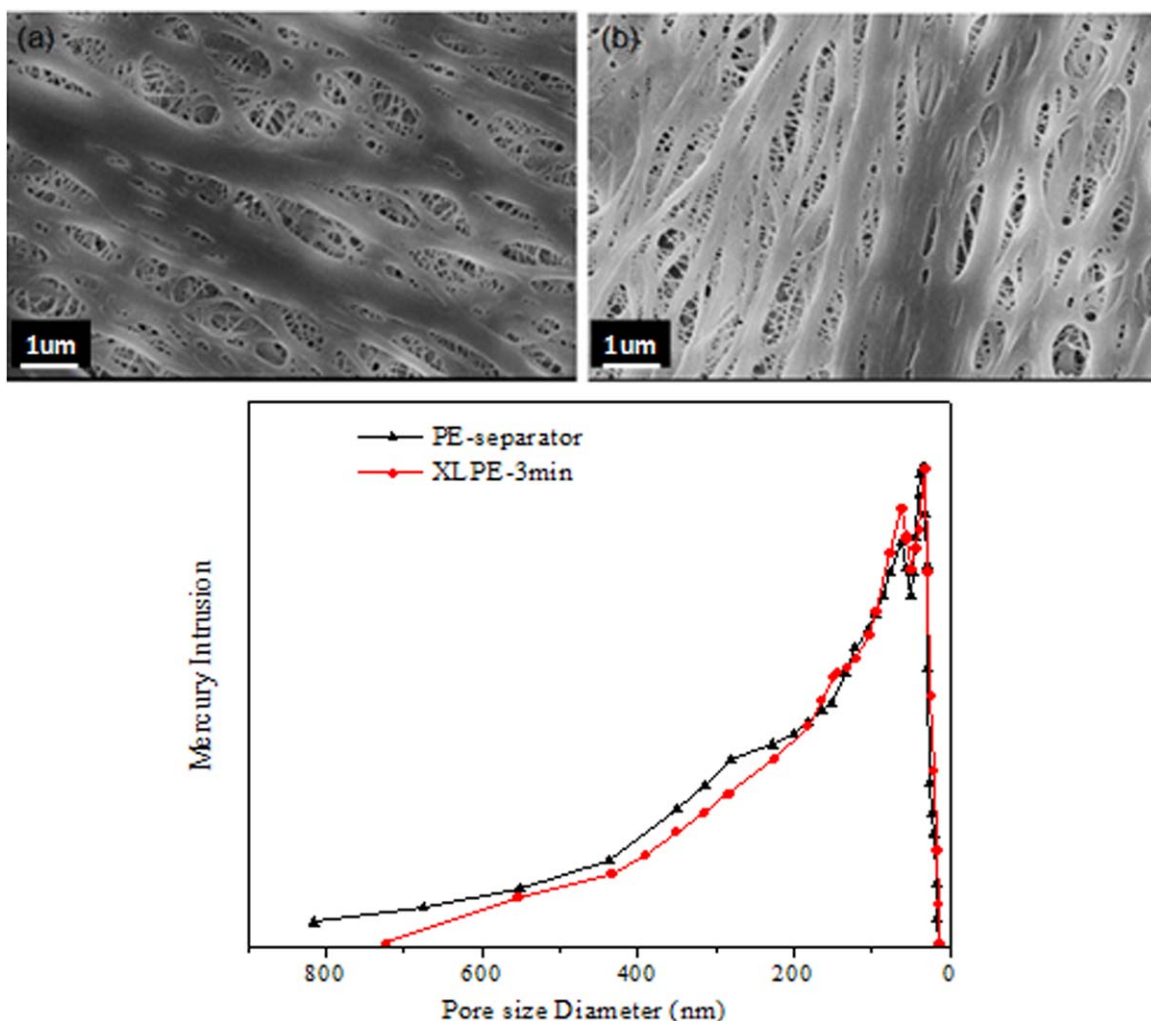


**Figure 2.** The SEMs and pore-size distribution of the commercial single-layer PE separator (PE) and the UV cross-linked PE separator (XL-PE) irradiated by 3 min. [Color figure can be viewed in the online issue, which is available at [wileyonlinelibrary.com](http://wileyonlinelibrary.com).]

of  $25 \pm 2^\circ$ . The elongation speed was 25 mm/min. Dumbbell-shaped specimens were prepared according to ASTM D412-87. Tensile strength and elongation at break were recorded.

**Infrared Spectroscopy Measurement.** The separator was measured by a Thermo Fisher Nicolet 5700 FTIR spectrometer by reflection method directly.

## RESULTS AND DISCUSSION

The low-cost PE single-layer separator would be desired if it could have good thermal stability. Inspired by PP/PE/PP triple-layer separator and ceramic-coated separator, the current work intends to modify the single-layer PE separator chain structure to enable it to have a similar composite structure to possess both auto-shutdown capacity and heat resistance temperature of higher than  $200^\circ\text{C}$ . To fulfill this task, the PE separator should have a highly cross-linked chain network to guarantee the integrity at high temperature. Meanwhile, enough uncross-linked polymer chain domains are also required to melt at around  $130^\circ\text{C}$  to fill the pores in the separator to realize the auto-

shutdown function. Besides, the treatment should have no effect on the porous structure of the PE separator.

In this study, the commercial single-layer microporous PE separator was chosen for further modification of polymer chain network to demonstrate the feasibility and efficiency of the proposed idea. The solid-state UV irradiation, operated at a temperature far below the PE melting temperature, can avoid the effect of irradiation on the porous structure of the PE

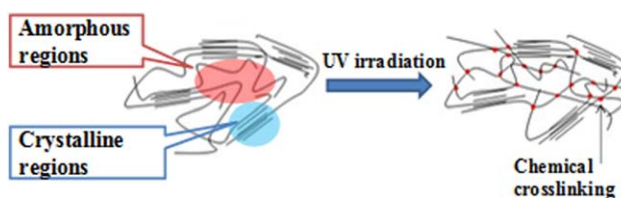


**Figure 3.** The schematic chain structure change of the PE separator through solid-state UV irradiation at low temperature. [Color figure can be viewed in the online issue, which is available at [wileyonlinelibrary.com](http://wileyonlinelibrary.com).]

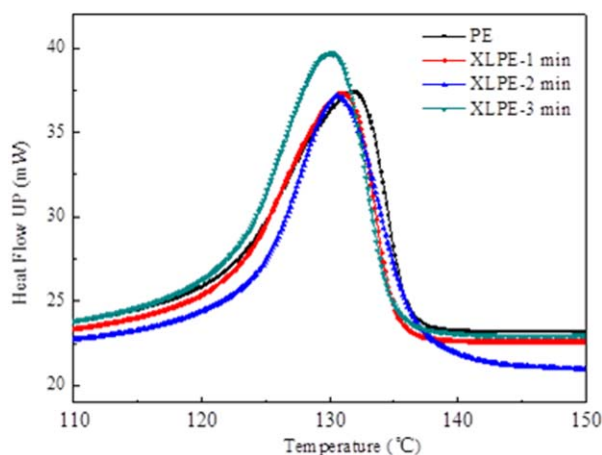


**Figure 4.** The DSC curves of the commercial single-layer PE separator (PE) and the UV cross-linked PE separator irradiated by 1 min (XLPE-1 min), 2 min (XLPE-2 min) and 3 min (XLPE-2 min), respectively. [Color figure can be viewed in the online issue, which is available at [wileyonlinelibrary.com](http://wileyonlinelibrary.com).]

separator and crystallized PE chains. Meanwhile, appropriate photoinitiator, cross-linker, and treatment method should be chosen to ensure the cross-linking efficiency after irradiation. Tremendous efforts were made to test various photoinitiators, cross-linkers, and treatment methods to achieve the best performance of the modified separator. In the optimized experimental procedure, the separator was first loaded with the additives by soaking it for 3 min in a methylene chloride solution containing 0.3 wt % benzophenone (photoinitiator) and 0.3 wt % triallylicyanurate (cross-linker) at room temperature. Then it was wiped and warmed to remove methylene chloride. UV lamp, instead of high energy irradiation source, was used in a UV cure reactor. The mercury lamp is 10 cm away from the surface of the separator. During the irradiation, the separator was submerged in the water to ensure the irradiation temperature controllable and keep separator isolated from oxygen.

As shown in Figure 2, the SEMs of the original PE separator and the partially cross-linked PE (XL-PE) separator after modification show that the solid-state UV irradiation has no influence on the morphology of the PE separator after current treatment method. The porosity measurements also demonstrated that there was no change in pore structure.

**Table I.** Melting Temperature and Corresponding Crystallinities of the Commercial Single-Layer PE Separator (PE) and the UV Cross-Linked PE Separator irradiated by 1 min (XLPE-1 min), 2 min (XLPE-2 min), and 3 min (XLPE-2 min), respectively.  $\Delta H_f^* = 287.3$  J/g

| Separator  | Irradiation time (min) | Melting peak (°C) | Heat of enthalpy (J/g) | Crystallinity (%) |
|------------|------------------------|-------------------|------------------------|-------------------|
| PE         | 0                      | 131.80            | 140.39                 | 48.3              |
| XLPE-1 min | 1                      | 130.97            | 131.92                 | 45.9              |
| XLPE-2 min | 2                      | 130.67            | 120.34                 | 41.9              |
| XLPE-3 min | 3                      | 130.00            | 113.74                 | 39.6              |

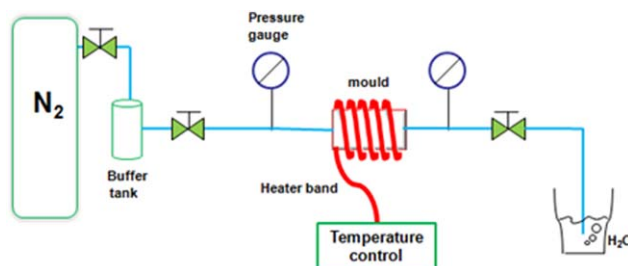


**Figure 5.** Separator permeability measurement setup. [Color figure can be viewed in the online issue, which is available at [wileyonlinelibrary.com](http://wileyonlinelibrary.com).]

To possess the auto-shutdown ability, enough uncross-linked PE chain domains must be maintained to melt at elevated temperature and fill the pores. This task can be fulfilled by the PE chains in crystallization domains. During the preparation of porous PE separator, enough crystallization domains have been generated to achieve porous structure through elongation. In current method, as illustrated in Figure 3, PE chains in crystallized status should be retained because during the solid-state UV irradiation process at low temperature, cross-linking will mainly happen to PE chains in amorphous domains.

The crystallinity was measured by DSC. The samples weighing about 4.0 mg were scanned in the temperature range of 20–200°C under nitrogen atmosphere with a heating rate of 10°C/min. The crystallinity was calculated using the following equation,

$$X_c = \frac{\Delta H_m}{\Delta H_m^0} \times 100$$

where  $X_c$  is the crystallinity,  $\Delta H_m$  is the specific enthalpy of melting, and  $\Delta H_m^0$  ( $=287.3$  J/g) is the specific melting enthalpy for 100% crystalline PE. The DSC results as shown in Figure 4

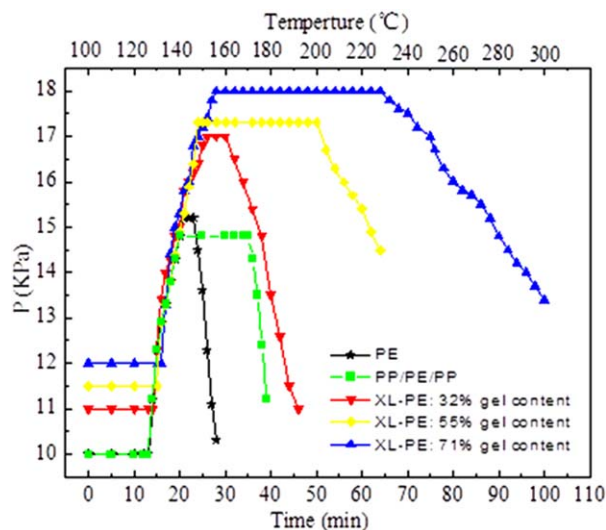


**Figure 6.** The gas permeability experiments of the commercial single-layer PE separator (PE), the commercial PP/PE/PP separator (PP/PE/PP), and the UV cross-linked PE separators (XL-PE) with different cross-linking densities. All the experiments were performed with same starting pressure of 10 KPa. In the figure, some curves are elevated arbitrarily for a clearer exhibition of data. [Color figure can be viewed in the online issue, which is available at [wileyonlinelibrary.com](http://wileyonlinelibrary.com).]



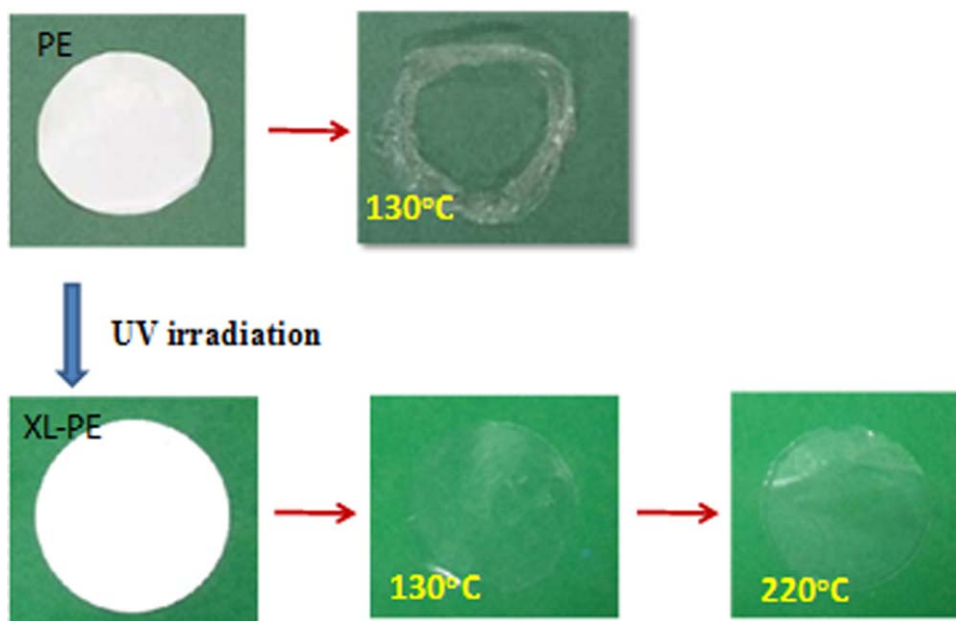


**Figure 7.** The heat resistance experiments of the commercial PE separator (PE) and the UV cross-linked PE separator (XL-PE). The separator was placed in a membrane holder with nitrogen gas flowing through it. The temperature of the holder was increasing at a rate of  $10^{\circ}\text{C}/\text{min}$ . [Color figure can be viewed in the online issue, which is available at [wileyonlinelibrary.com](http://wileyonlinelibrary.com).]

and Table I show the crystallinity of the original commercial PE separator was around 48%, which is believed to be enough to fulfill the task of auto-shutdown. As a result, the irradiation conditions were optimized to achieve the highest cross-linking degree without affecting the separator morphology to increase its thermal stability. With these prerequisites, the highest gel content achieved in current work is 71%. The DSC measurement shows after the irradiation that the crystallinity decreased to 39.6%, which demonstrated most crystallized PE domains were remained. As a result, a PE separator with composite structure was achieved.

To test the auto-shutdown and thermal stability of the separators, gas permeability experiment was carried out as shown in Figure 5. The separator was placed in a membrane holder with nitrogen gas flowing through it. The separator was supported by two thin 200 mesh stainless-steel nets and put into the membrane holder. Heater strap was wrapped around the holder and

the pipes before the membrane holder to control the temperature. Nitrogen flew from the left of the mold to the right. The pressure was read from the pressure gauge. The end of the pipe was submerged in water to observe the air flow. The temperature of the holder was increasing at a rate of  $10^{\circ}\text{C}/\text{min}$ .

When the temperature of the holder was increased to  $130^{\circ}\text{C}$ , as shown in Figure 6, the commercial PE separator started to melt and lose its porous structure, so the upper pressure of the holder increased and the gas flow stopped. However, within 1 min, the upper pressure decreased and the gas flew freely through the membrane holder indicating the failure of the PE separator. As shown in Figure 7, the commercial PE separator falls entirely. Regarding the partially cross-linked PE separator, it has the auto-shutdown capacity at the same temperature of  $130^{\circ}\text{C}$  as the commercial PE separator. The gas flow stopped immediately and the upper pressure increased quickly at  $130^{\circ}\text{C}$ . It demonstrated that  $\sim 40\%$  crystallized PE chains are sufficient

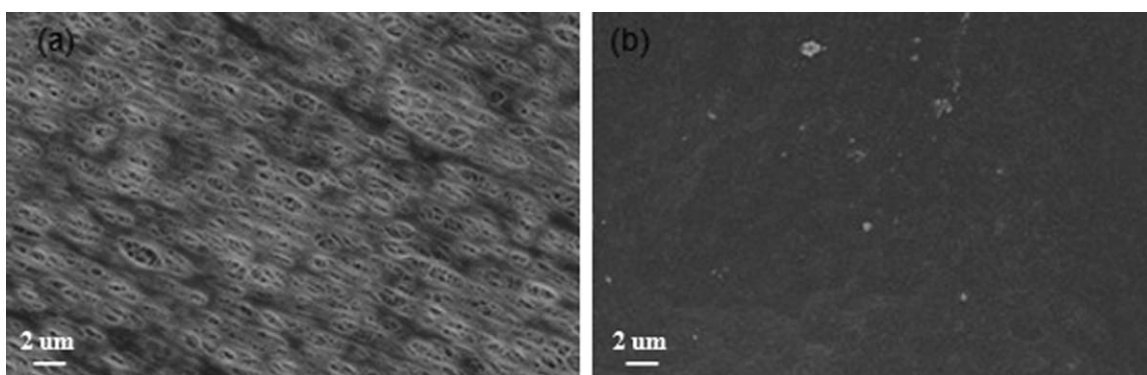


**Figure 8.** The morphology change of the UV irradiated PE separator at  $130^{\circ}\text{C}$ . (a) The original PE separator and (b) the PE separator after heating at  $130^{\circ}\text{C}$ .

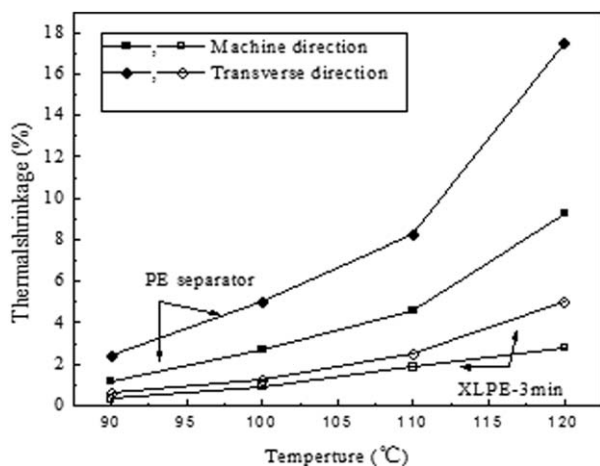


**Figure 9.** The thermal shrinkage of the commercial single-layer PE separator (PE) and the UV cross-linked PE separator irradiated by 3 min (XLPE-3 min) after leaving them freely in an oven at 90~120°C for 10 min.

to fulfill the auto-shutdown task and the shutdown temperature is unaffected. The SEM results, as in Figure 8, show that at 130°C all the pores disappeared. The transparency of the melted PE separator also indicated the loss of its porous structure as shown in Figure 7. With the increase of temperature, the partially cross-linked PE separator with a gel content of 71% can hold until 220°C, then the upper pressure started dropping and small air flow was observed. As shown in Figure 7, at this temperature, the modified PE separator can still maintain its integrity. There are only some micropores leading to the small air flow and the pressure drop. This integrity is very important in the lithium-ion battery to avoid the large area direct contact of electrodes and the uncontrollable increase of temperature. To make a comparison, a commercial PP/PE/PP separator was also studied under this system. The results showed it has the auto-shutdown capacity at 130°C, but loses its integrity at around 170°C, which is around the melting temperature of PP. The current heat resistance capacity shown by XL-PE is high enough to

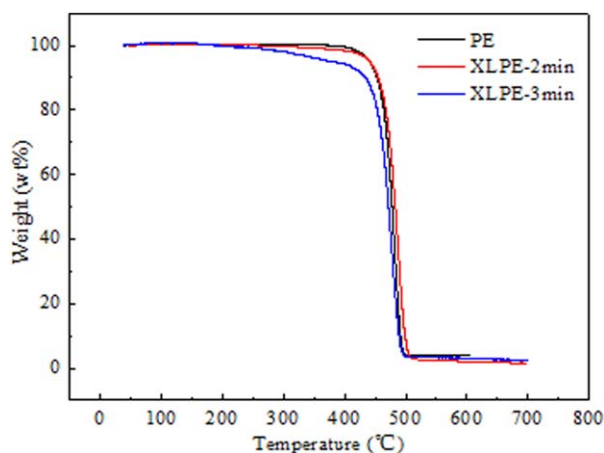


**Figure 10.** TGA thermogram of the commercial single-layer PE separator (PE) and the UV cross-linked PE separator irradiated by 2 min (XLPE-2 min) and 3 min (XLPE-3 min), respectively. [Color figure can be viewed in the online issue, which is available at [wileyonlinelibrary.com](http://wileyonlinelibrary.com).]

hold the integrity at special conditions. Besides, it has the auto-shutdown capacity. The safety window is around 90°C.

The influence of this partially cross-linked structure on other properties of the PE separator was also studied to make sure the current modified chain structure can meet various requirements of separator for lithium-ion battery. The thermal shrinkage of the separators was measured because it is another important parameter determining the safety under the elevated temperature. The shrinkage of the separator at elevated temperature must be low to avoid the contact of electrodes. The changes in the dimensions on both machine direction (MD) and transverse direction (TD) after leaving the separator freely in an oven at 90~120°C for 10 min were measured. As shown in Figure 9, the thermal shrinkage of the PE separator decreased gradually with increased cross-linking level. Because in the XL-PE separator a cross-linked network forms which prevents the shrinkage of the PE chains, the PE separator is more difficult to shrink with the increase of gel content, which increases the safety of lithium-ion battery. As shown in Figure 10, the thermal degradation performance of the XL-PE separator with 70% gel content is a little worse than the original PE separator due to the UV irradiation, but it is still stable till 250°C, which is high enough for the application for electric vehicles. The modified PE separator with 53% gel content has the same thermal degradation behavior as the untreated PE separator.

The mechanical properties of XL-PE separators with different gel contents were also measured. As shown in Figures 11 and 12, with the increase of gel content from 32 to 71%, the Young's modulus increased attributed to the cross-linking. However, the elongation at the break decreased from 35.8 to 13.5%. The tensile strength decreased as well. This is because the cross-linking network increased the rigidity, thereby preventing the stretching of polymer chains. However, these values still meet the requirements from the separator for lithium-ion battery. Nevertheless, the decrease of tensile strength might decrease the safety of battery cells during fierce accidents.

Another important property improvement brought by the irradiation was the hydrophilicity. It is well known the

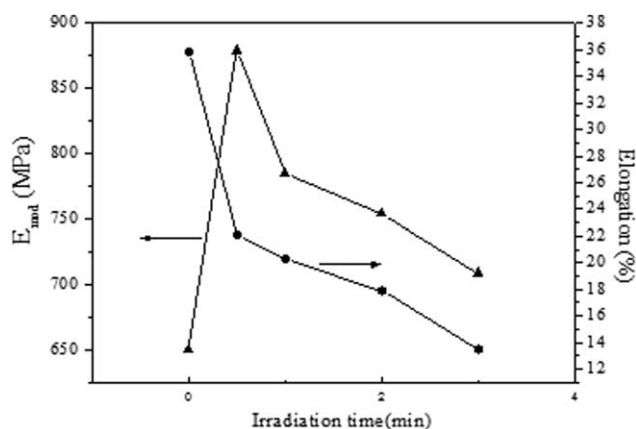


**Figure 11.** The modulus and elongation change of the commercial single-layer PE separator and the UV cross-linked PE separator irradiated by different times.

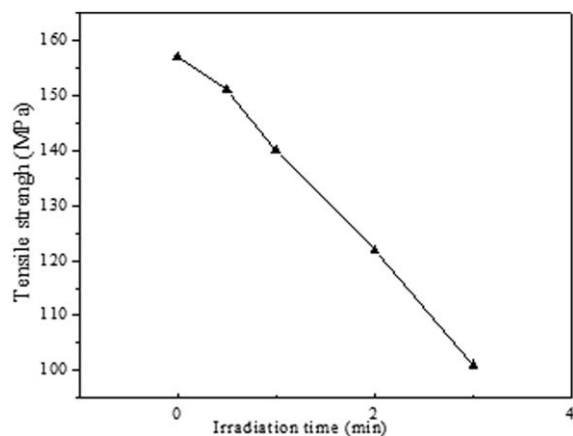


**Figure 12.** The tensile strength change of the commercial single-layer PE separator and the UV cross-linked PE separator irradiated by different times.

hydrophobicity is one of the disadvantages of polyolefin separators because the organic electrolyte solution is polar.<sup>21,22</sup> The hydrophobic olefin separator affects the adsorption of the electrolyte into its pores giving low battery power, which is one of the problems especially for the application in electric vehicles. As a result, surface modification is sometimes necessary to increase the hydrophilicity of the PE separator aimed at a higher adsorption ability of the electrolyte. However, this further modification will bring extra cost to the PE separator and may affect the PE separator property. In current method, the surface was changed into hydrophilic by the irradiation, resolving this problem simultaneously. As shown in Figure 13, the contact angle measurements of the PE and XL-PE separators show the XL-PE separator has very good hydrophilicity after the irradiation. It is because of the introduction of hydrophilic groups to the PE separator during the UV irradiation. As shown in Figure 14, the infrared spectra of the PE and XL-PE separators were compared. After the irradiation, new bands appeared at  $1780\sim 1550\text{ cm}^{-1}$ . The bands near

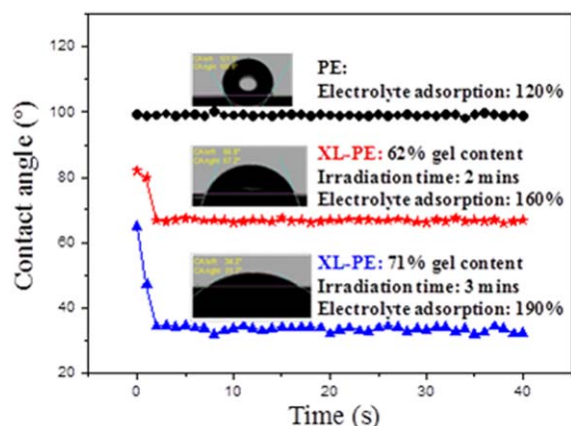


**Figure 13.** The water contact angle and the electrolyte adsorption of the commercial single-layer PE separator (PE) and the UV cross-linked PE separator (XL-PE) with different cross-linking densities. [Color figure can be viewed in the online issue, which is available at [wileyonlinelibrary.com](http://wileyonlinelibrary.com).]

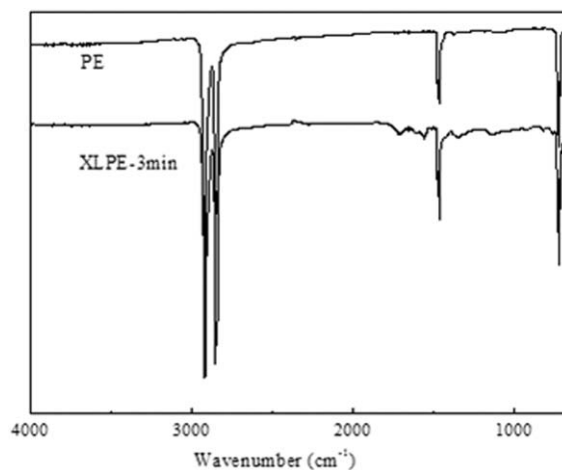


**Figure 14.** FTIR spectra of the commercial single-layer PE separator (PE) and the UV cross-linked PE separator irradiated by 3 min (XLPE-3 min).

$1708\text{ cm}^{-1}$  indicated carbonyl (C=O) group and  $1560\text{ cm}^{-1}$  corresponded to amide band due to the group from triallylcyanurate grafted onto the PE separator, respectively. Thus, the presence of hydrophilic groups on the XL-PE separator gave them hydrophilic surface so the separator can be wetted more sufficiently in the electrolyte. As shown in Figure 15, the electrolyte adsorption measurements show that after the irradiation the highest adsorption quantity of the electrolyte was increased from 120% to 190%. As shown in Figure 16, when the electrolyte was poured onto the PE separator, small air bubbles generated on the surface of the commercial PE separator, while the electrolyte can wet the XL-PE separator very well. The quick absorption of electrolyte into the separator is greatly preferred during the manufacture of battery cells. However, it may not bring extra improvement to cell performance. If only enough electrolyte has been absorbed and certain ion conductivity is reached, the cell performance should be similar.

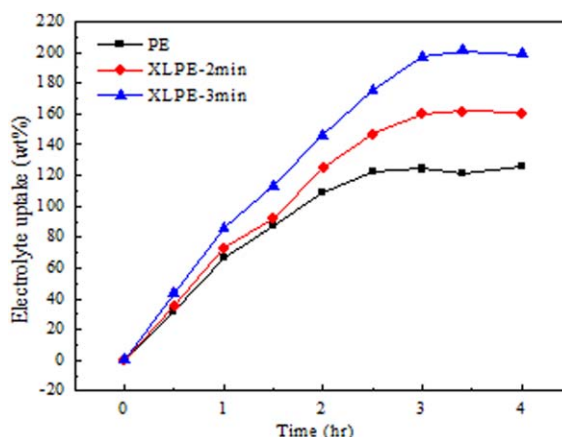


**Figure 15.** The uptake behavior of the liquid electrolyte for the commercial single-layer PE separator (PE) and the UV cross-linked PE separator irradiated by 2 min (XLPE-2 min) and 3 min (XLPE-3 min), respectively. [Color figure can be viewed in the online issue, which is available at [wileyonlinelibrary.com](http://wileyonlinelibrary.com).]

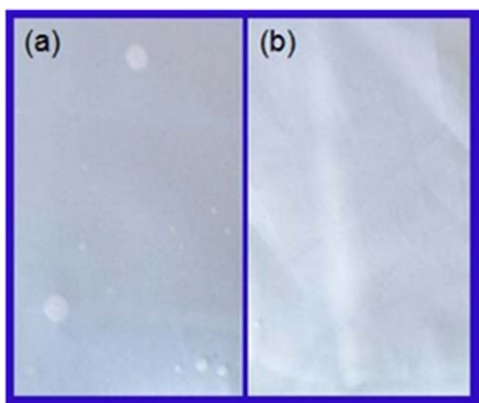


**Figure 16.** Photographs of (a) the commercial single-layer PE separator (PE) and (b) the UV cross-linked PE separator irradiated by 3 min (XLPE-3 min) after pouring EC/DMC solution with 1M LiPF<sub>6</sub> in it on the surface of the separators. [Color figure can be viewed in the online issue, which is available at [wileyonlinelibrary.com](http://wileyonlinelibrary.com).]

## CONCLUSIONS

In summary, this article demonstrated that the single-layer PE separator could have both auto-shutdown capacity and satisfactory thermal stability after its chain structure is modified. The heat resistance temperature can be as high as 220°C. The modified PE separator is hydrophilic and able to absorb much more electrolyte. Considering the low cost and the easy preparation of current partially cross-linked PE separator, it could become a new choice as the separator for lithium-ion batteries for various applications, including electric vehicles and energy storage purpose.

This article employed a commercial PE separator to demonstrate that a single-layer PE separator with modified chain structure can have satisfactory performance meeting severe requirements for lithium-ion battery separator. In practical, the UV treatment method to obtain this composite structure could vary. In our industrial-scale design, appropriate initiator and cross-linker can be introduced with the raw PE materials at very begin to skip the later soaking process. The irradiation can be conducted in inert gas atmosphere. Mercury lamp with certain wavelength, instead of the high-pressure mercury lamp, is used to decrease cost. We have modified our PE separator producing process to make it more suitable for this technology. The shrinkage of the separator produced by ourselves is undetectable at the transverse direction even at the temperature of 220°C after UV treatment.

## ACKNOWLEDGMENTS

The authors would like to thank the financial support from National Natural Science Funds for Distinguished Young Scholar (Grant No. 21125626), National Natural Science Foundation of China (Grant No. 21374096, 21106128), Science and Technology

Project of Zhejiang Province (Grant No.2012F20007), and the Open Project from The State Key Laboratory of Chemical Engineering (SKL-ChE-10D06).

## REFERENCES

1. Woo, J. J.; Zhang, Z. C.; Amine, K. *Adv. Energy Mater.* **2014**, *4*, 1301208.
2. Shi, J. L.; Hu, H. S.; Xia, Y. G.; Liu, Y. Z.; Liu, Z. P. *J. Mater. Chem. A* **2014**, *2*, 9134.
3. Wei, X. L.; Nie, Z. M.; Luo, Q. T.; Li, B.; Chen, B. W.; Simmons, K.; Sprenkle, V.; Wang, W. *Adv. Energy Mater.* **2013**, *3*, 1215.
4. Balakrishnan, P. G.; Ramesh, R.; Kumar, T. P. *J. Power Sources* **2006**, *155*, 401.
5. Shi, J. L.; Fang, L. F.; Li, H.; Zhang, H.; Zhu, B. K.; Zhu, L. P. *J. Membr. Sci.* **2013**, *437*, 160.
6. Zhang, S. S. *J. Power Sources* **2007**, *164*, 351.
7. Arora, P.; Zhang, Z. M. *Chem. Rev.* **2004**, *104*, 4419.
8. Huang, X. S. *J. Solid State Electrochem.* **2011**, *15*, 649.
9. Huang, X. S.; Hitt, J. J. *J. Membr. Sci.* **2013**, *425*, 163.
10. Lalia, B. S.; Samad, Y. A.; Hashaikeh, R. *J. Appl. Polym. Sci.* **2012**, *126*, E441.
11. Gwon, H.; Hong, J.; Kim, H.; Seo, D. H.; Jeon, S.; Kang, K. *Energy Environ. Sci.* **2014**, *7*, 538.
12. Prasanna, K.; Kim, C. S.; Lee, C. W. *Mater. Chem. Phys.* **2014**, *146*, 545.
13. Zhao, L. L.; Zhu, Y. P.; Wang, X. Y. *J. Inorg. Mater.* **2013**, *28*, 1296.
14. Raja, M.; Angulakshmi, N.; Thomas, S.; Kumar, T. P.; Stephan, A. M. *J. Membr. Sci.* **2014**, *471*, 103.
15. Liu, H. Y.; Xu, J.; Guo, B. H.; He, X. M. *J. Appl. Polym. Sci.* **2014**, 131.
16. Khonakdar, H. A.; Morshedian, J.; Wagenknecht, U.; Jafari, S. H. *Polymer* **2003**, *44*, 4301.
17. Sohn, J. Y.; Gwon, S. J.; Choi, J. H.; Shin, J.; Nho, Y. C. *Nucl. Instrum. Methods Phys. Res. Sect B Beam Interact. Mater. Atoms* **2008**, *266*, 4994.
18. Sohn, J. Y.; Lim, J. S.; Gwon, S. J.; Shin, J.; Choi, J. H.; Nho, Y. C. *Polym. Korea* **2008**, *32*, 598.
19. Im, J. S.; Sohn, J. Y.; Shin, J.; Lim, Y. M.; Choi, J. H.; Kim, J. S.; Nho, Y. C. *Polym. Korea* **2010**, *34*, 74.
20. Park, J. S.; Cho, I. H.; Gwon, S. J.; Lim, Y. M.; Nho, Y. C. *Radiat. Phys. Chem.* **2009**, *78*, 501.
21. Wang, D.; Zhao, Z. L.; Yu, L. N.; Zhang, K. J.; Na, H.; Ying, S. Q.; Xu, D. C.; Zhang, G. J. *J. Appl. Polym. Sci.* **2014**, 131.
22. Lee, H.; Alcoutlabi, M.; Watson, J. V.; Zhang, X. W. *J. Appl. Polym. Sci.* **2013**, *129*, 1939.